Available online at www.sciencedirect.com
SCIENCE DIRECT®
International Journal of Heat and Mass Transfer 47 (2004) 2501–2509
International Journal of HEAT and MASS TRANSFER
www.elsevier.com/locate/ijhmt

Technical Note

Numerical resolution of the radiative transfer equation in a cylindrical enclosure with the finite-volume method

M. Ben Salah *, F. Askri, K. Slimi, S. Ben Nasrallah

Ecole Nationale d'Ingénieurs de Monastir, Laboratoire d'Etudes des, Systèmes Thermiques et Energétiques (LESTE), Rue Ibn Eljazzar, 5019 Monastir, Tunisia

Received 12 March 2002

Abstract

The radiative transfer equation is solved by the finite-volume method in an axisymmetric two-dimensional geometry with absorbing, emitting, and either isotropically or anisotropically scattering gray medium. Explicit expressions of the coefficients appearing in the discretized angular redistribution term have been determined. These coefficients verify the recursive relation established by Carlson and Lathrop [Greenspan, Kelber, Okrent (Eds.), Computing Method in Reactors Physics, Gordon and Breach, New York, 1968, p. 171] and lead to accurate numerical results.

1. Introduction

The axisymmetric radiative transfer in cylindrical enclosure has been studied extensively due to its geometric simplicity and practical engineering applications to gas turbine combustors, heat pipes, nuclear reactors safety and pulverized coal combustors. During the past few decades, numerous methods have been proposed to solve the radiative transfer equation (RTE), which is integro-differential equation in nature (Monte Carlo method [1], flux method [2], zones method [3], Galerkine method [4], Harmonic spherical method [5], method of solution based on using appropriate expansion functions [6], discrete ordinates method, MOD [7,8] and the finite-volume method (FVM) [9–13]).

The axisymmetric RTE includes a partial derivative with respect to an angular coordinate, typically referred to as an angular redistribution term (ART) of radiative energy. Following the artifice of Carlson and Lathrop [14], which maintains neutron conservation and permits minimal direction coupling, among other works using the DOM, Fiveland [7], Jendoubi et al. [8] and Jamaluddin and Smith [15] have used a recursive relation for the numerical treatment of this term. The recursive relation determined by [14] has been also used by Baek and Kim [13] to develop a modified discrete ordinates method (MDOM) in order to study radiative transfer in an axisymmetric cylindrical enclosure.

A FVM has been used by Chui and Raithby [9] to compute radiant heat transfer on a nonorthogonal, boundary-fitted meshes. To solve three-dimensional radiation problems in cylindrical enclosures, Chui et al. [10] have implemented a FVM and present a mapping for solution of axisymmetric problems by solving the intensity in a single azimuthal direction. The FVM for computing radiative heat transfer has been extended to domains with periodic boundaries by Mathur and Murthy [16]. The authors have used a new technique to account for control angle overhang, and to correctly redistribute radiant energy at rotationally periodic boundaries. An unstructured FVM for radiative heat transfer has been developed by Liu et al. [17] and they are applicable for 2D planar, axisymmetric and 3D problems with structured, unstructured, or hybrid grids. For a 2D axisymmetric problem, the authors have employed the recursive relation developed by [14] to treat the angular derivative term.

* Corresponding author.

0017-9310/$ - see front matter © 2003 Elsevier Ltd. All rights reserved.
doi:10.1016/j.ijheatmasstransfer.2003.11.023

Nomenclature

A_e, A_w, A_t, A_b surface area, m^2
D_{cr}^{mn} radial directional weights
E emissive power ($= \sigma T^4$), $W\,m^{-2}\,sr^{-1}$
H cylinder height, m
I actual radiative intensity, $W\,m^{-2}\,sr^{-1}$
I^0 blackbody radiative intensity, $W\,m^{-2}\,sr^{-1}$
κ_a absorption coefficient, m^{-1}
κ_s scattering coefficient, m^{-1}
κ_e extinction coefficient, m^{-1}
κ_{em} modified extinction coefficient, m^{-1}
N_r, N_z radial and axial nodal number
N_θ, N_ψ polar and azimuthal angle number
Q^r dimensionless radiative heat flux
q^r radiative heat flux, $W\,m^{-2}$
R cylinder radius, m
r, z distance along radial and axial direction, m
r_c cylinder radius, m
z_c cylinder height, m
S source term (Eq. (2))
T temperature, K

Greek symbols

$\alpha_{mn\pm\frac{1}{2}}$ coefficients of the angular derivative term
ε emissivity
D_{cz}^{mn} axial directional weights
Δr, Δz radial and axial steps
$\Delta\theta$, $\Delta\psi$ polar and azimuthal steps
$\Delta\Omega^{mn}$ discrete control (solid) angle
σ Stefan–Boltzmann constant ($= 5.67\times10^{-8}$ $W\,m^{-2}\,K^{-4}$)
τ optical thickness ($= \kappa_a r_c$)
θ_P scattering angle
$\vec{\Omega}$, $\vec{\Omega}'$ outward and inward radiation directions
Φ scattering phase function
μ, η, ξ direction cosines

Subscripts

b blackbody
c cold, cylinder
g gas
h hot
E, W, T, B east, west, top, and bottom neighbors nodal points of P
e, w, t, b east, west, top, and bottom control volume faces
P nodal point in which intensities are located
r related to the r-axis
z related to the z-axis
w wall

Superscripts

0 blackbody
m, n, m', n' radiation direction
r radiative quantity

For our knowledge, no rigorous explanation of this recursive relation has been presented. One intends, in the present paper, to affirm the validity of this relation by the determination of the explicit expressions of the coefficients intervening in the discretized ART while using the FVM and to validate the numerical results obtained using the determined expressions by comparison with existing results.

The remainder of this article is divided into three sections. The governing equations and the discretized equations are firstly presented. This is followed by a comparison of the present method (FVM) with other available methods. Finally some concluding remarks and an Appendix A are presented.

2. Mathematical formulation

Radiative heat transfer in a gray semi-transparent medium is governed by the following equation [18]:

$$\left.\frac{dI}{ds}\right|_{\vec{\Omega}} = -\kappa_e(\vec{r})I(\vec{r},\vec{\Omega}) + S(\vec{r},\vec{\Omega}) \tag{1}$$

with

$$S = \kappa_a(\vec{r})I^0(\vec{r}) + \frac{\kappa_s(\vec{r})}{4\pi}\int_{4\pi} I(\vec{r},\vec{\Omega}')\Phi(\vec{\Omega}'\to\vec{\Omega})\,d\Omega' \tag{2}$$

where $\vec{\Omega}$ is the direction of propagation defined as:

$$\vec{\Omega} = \mu\vec{e}_r + \eta\vec{e}_\varphi + \xi\vec{e}_z$$

and (μ, η, ξ) are the direction cosines expressed as follows:

$$(\mu = \sin\theta\cos\psi, \eta = \sin\theta\sin\psi, \xi = \cos\theta)$$

(θ, ψ) are respectively, the polar angle and the azimuthal angle defining the direction of propagation $\vec{\Omega}$ (Fig. 1).

In the case of axisymmetric radiative transfer, Eq. (1) is expressed in cylindrical coordinates as follows:

$$\frac{1}{r}\frac{\partial}{\partial r}(r\mu I)\bigg|_{(\varphi,z,\theta,\psi)} + \frac{\partial}{\partial z}(\xi I)\bigg|_{(r,\varphi,\theta,\psi)} \frac{1}{r}\frac{\partial}{\partial\psi}(\eta I)\bigg|_{(r,\varphi,z,\theta)} = -\kappa_e I + S(\vec{r},\vec{\Omega}) \tag{3}$$

In Eq. (3), it appears a supplementary term regardless the RTE expression in cartesian coordinates, namely

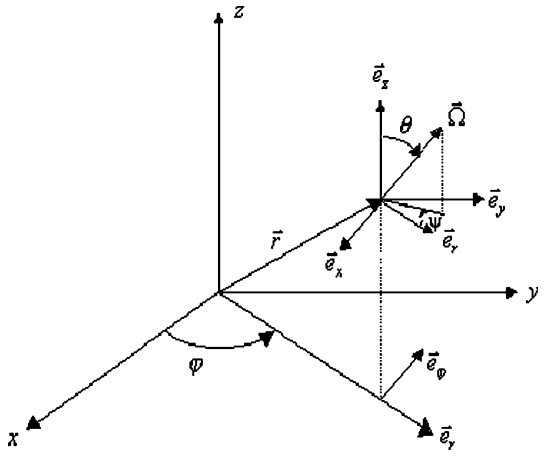

Fig. 1. Angular coordinate (θ, ψ) of the direction $\vec{\Omega}$ defined in the cylindrical base $(\vec{e}_r, \vec{e}_\varphi, \vec{e}_z)$.

called angular redistribution term (ART), whose expression is as follows:

$$\mathrm{ART} \equiv -\frac{1}{r}\frac{\partial}{\partial\psi}(\eta I)\bigg|_{(r,\varphi,z,\theta)} \tag{4}$$

3. Numerical procedure

Eq. (3) is solved numerically by the FVM [19]. The spatial domain is subdivided in $N_r \times N_z$ spatial control volumes (Fig. 2) where:

$$\Delta r = \frac{R}{N_r} \quad \text{and} \quad \Delta z = \frac{H}{N_z}$$

R and H are respectively, the radius and the height of the cylindrical enclosure and Δr and Δz are, respectively r and z space steps:

$$\Delta r = r_\mathrm{e} - r_\mathrm{w}; \quad \Delta Z = z_\mathrm{t} - z_\mathrm{b}$$

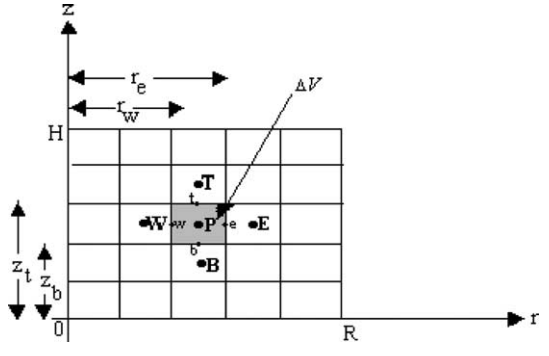

Fig. 2. Spatial control volume in the r–z plane.

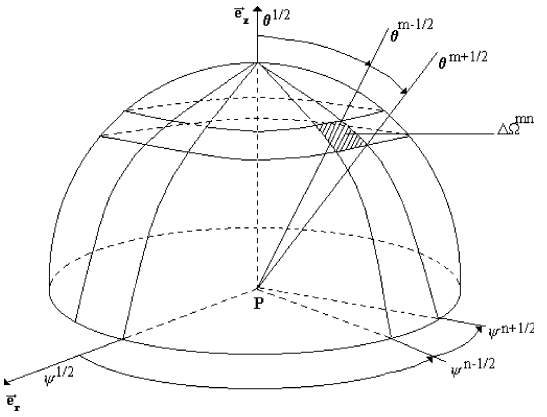

Fig. 3. Control solid angle.

The total solid angle ($\Omega = 4\pi\,\mathrm{str}$) is subdivided in $N_\theta \times N_\psi$ control solid angles, where $\Delta\theta = \frac{\pi}{N_\theta}$. and $\Delta\psi = \frac{2\pi}{N_\psi}$.

$\Delta\theta$ and $\Delta\psi$ are respectively θ and ψ steps: $\Delta\theta = \theta^{m+\frac{1}{2}} - \theta^{m-\frac{1}{2}}$; $\Delta\psi = \psi^{n+\frac{1}{2}} - \psi^{n-\frac{1}{2}}$.

The control angle $\Delta\Omega^{mn}$ is defined (Fig. 3) by the angular range $\lfloor \theta^{m+\frac{1}{2}} = m\Delta\theta; \theta^{m-\frac{1}{2}} = (m-1)\Delta\theta \rfloor$ and $\lfloor \psi^{n+\frac{1}{2}} = n\Delta\psi; \psi^{n-\frac{1}{2}} = (n-1)\Delta\psi \rfloor$:

$$\Delta\Omega^{mn} = \int_{\theta^{m-\frac{1}{2}}}^{\theta^{m+\frac{1}{2}}} \int_{\psi^{n-\frac{1}{2}}}^{\psi^{n+\frac{1}{2}}} \sin\theta\,\mathrm{d}\theta\,\mathrm{d}\psi$$

The radiative intensity at a point P and in the direction (θ^m, ψ^n) is represented by I_P^{mn}. The integration of Eq. (3) over the control volume Δv and the control angle $\Delta\Omega^{mn}$ gives:

$$\underbrace{\int_{\Delta v}\int_{\Delta\Omega^{mn}} \frac{1}{r}\frac{\partial}{\partial r}(Ir\sin\theta\cos\psi)\,\mathrm{d}v\,\mathrm{d}\Omega}_{\text{(a)}} + \underbrace{\int_{\Delta v}\int_{\Delta\Omega^{mn}} \frac{\partial}{\partial z}(I\cos\theta)\,\mathrm{d}v\,\mathrm{d}\Omega}_{\text{(b)}} - \underbrace{\int_{\Delta v}\int_{\Delta\Omega^{mn}} \frac{1}{r}\frac{\partial}{\partial\psi}(I\sin\theta\sin\psi)\,\mathrm{d}v\,\mathrm{d}\Omega}_{\text{(c)}} = \underbrace{\int_{\Delta v}\int_{\Delta\Omega^{mn}} (-\kappa_\mathrm{e} I + S(\vec{r},\vec{\Omega}))\,\mathrm{d}v\,\mathrm{d}\Omega}_{\text{(d)}} \tag{5}$$

The development of terms (a), (b) and (c) leads to (Appendix A):

$$(\mathrm{a}) = D_{cr}^{mn}(A_\mathrm{e} I_\mathrm{e}^{mn} - A_\mathrm{w} I_\mathrm{w}^{mn}) \tag{6}$$

$$(\mathrm{b}) = D_{cz}^{mn}(A_\mathrm{t} I_\mathrm{t}^{mn} - A_\mathrm{b} I_\mathrm{b}^{mn}) \tag{7}$$

A_b, A_t, A_w, A_e are the areas of bottom, top, west and east faces of the control volume Δv, respectively, and D_{cr}^{mn} and

D_{cz}^{mn} are the direction cosines regarding the r and z directions, respectively.

$$A_t = A_b = \pi(r_e^2 - r_w^2), \quad A_e = 2\pi\Delta z r_e, \quad A_w = 2\pi\Delta z r_w$$

$$D_{cz}^{mn} = \int_{\Delta\Omega^{mn}} (\vec{\Omega}\cdot\vec{e}_z)\,d\Omega \tag{8a}$$

$$D_{cr}^{mn} = \int_{\Delta\Omega^{mn}} (\vec{\Omega}\cdot\vec{e}_r)\,d\Omega \tag{8b}$$

$$(c) = (A_e - A_w)(\alpha_{mn+1/2} I_P^{mn+1/2} - \alpha_{mn-1/2} I_P^{mn-1/2}) \tag{9}$$

where

$$\alpha_{mn+\frac{1}{2}} = -\sin(\psi^{n+1/2})\left\{\frac{\Delta\theta}{2} - \frac{1}{4}[\sin(2\theta^{m+1/2}) - \sin(2\theta^{m-1/2})]\right\} \tag{10a}$$

$$\alpha_{mn-\frac{1}{2}} = -\sin(\psi^{n-1/2})\left\{\frac{\Delta\theta}{2} - \frac{1}{4}[\sin(2\theta^{m+1/2}) - \sin(2\theta^{m-1/2})]\right\} \tag{10b}$$

The discretized angular redistribution is written, in the same form as by Carlson and Lathrop [14] in the same form and the coefficients $\alpha_{mn+1/2}$ and $\alpha_{mn-1/2}$ are determined by a recursive relation based on the condition of radiative energy conservation:

$$\alpha_{mn+\frac{1}{2}} - \alpha_{mn-\frac{1}{2}} = D_{cr}^{mn} \tag{11a}$$

$$\alpha_{m\frac{1}{2}} = 0 \tag{11b}$$

It can be easily shown that these recursive relations are verified by the established expressions (Eqs. (10a) and (10b)):

$$\begin{aligned}\alpha_{mn+\frac{1}{2}} - \alpha_{mn-\frac{1}{2}} &= -\left\lfloor \frac{\Delta\theta}{2}\frac{1}{4}(\sin 2\theta^{m+\frac{1}{2}} - \sin 2\theta^{m-\frac{1}{2}})\right\rfloor(\sin\psi^{n+\frac{1}{2}} - \sin\psi^{n-\frac{1}{2}}) \\ &= \int_{\psi^{n-\frac{1}{2}}}^{\psi^{n+\frac{1}{2}}} \cos\psi\,d\psi \int_{\theta^{m-\frac{1}{2}}}^{\theta^{m+\frac{1}{2}}} \left(\frac{1+\cos 2\theta}{2}\right)d\theta \\ &= \int_{\psi^{n-\frac{1}{2}}}^{\psi^{n+\frac{1}{2}}} \cos\psi\,d\psi \int_{\theta^{m-\frac{1}{2}}}^{\theta^{m+\frac{1}{2}}} \sin^2\theta\,d\theta \\ &= \int_{\psi^{n-\frac{1}{2}}}^{\psi^{n+\frac{1}{2}}} \int_{\theta^{m-\frac{1}{2}}}^{\theta^{m+\frac{1}{2}}} \cos\psi\sin^2\theta\,d\theta\,d\psi = D_{cr}^{mn}\end{aligned}$$

$$\alpha_{m\frac{1}{2}} = -\sin(0)\left\{\frac{\Delta\theta}{2}\frac{1}{4}[\sin(2\theta^{m+\frac{1}{2}}) - \sin(2\theta^{m-\frac{1}{2}})]\right\} = 0$$

The development of term (d) leads to (Appendix A):

$$(d) = -\kappa_e \Delta v\,\Delta\Omega^{mn} I_P^{mn} + S_P^{mn}\,\Delta v\,\Delta\Omega^{mn} \tag{12}$$

where

$$S_P^{mn} = \frac{\kappa_s}{4\pi} I_P^{mn}\overline{\Phi}_{mnmn}\,\Delta\Omega^{mn} + S_{mp}^{mn} \tag{13a}$$

$$S_{mp}^{mn} = \kappa_a I_P^0(T) + \frac{\kappa_e}{4\pi}\sum_{(m'n')\neq(m,n)} I_P^{m'n'}\overline{\Phi}^{m'n'mn}\,\Delta\Omega^{m'n'} \tag{13b}$$

$$\overline{\Phi}^{m'n'mn} = \frac{1}{\Delta\Omega^{mn}\Delta\Omega^{m'n'}}\int_{\Delta\Omega^{m'n'}}\int_{\Delta\Omega^{mn}} \Phi(\vec{\Omega}'\to\vec{\Omega})\,d\Omega\,d\Omega' \tag{13c}$$

In order to overcome the convergence problem of the numerical solution, due to the discretization of the phase function that must verify the normalization condition ($\frac{1}{4\pi}\sum_{m'n'}\Phi^{mnm'n'}\Delta\Omega^{m'n'} = 1$), a correction coefficient γ is used. This coefficient is obtained such:

$$\frac{1}{4\pi}\sum_{m'n'}(1+\gamma)\Phi^{mnm'n'}\,\Delta\Omega^{m'n'} = 1 \tag{14a}$$

Then

$$\gamma = \frac{1}{\frac{1}{4\pi}\sum_{m'n'}\Phi^{mnm'n'}\,\Delta\Omega^{m'n'}} - 1 \tag{14b}$$

The function $\overline{\Phi}^{m'n'mn}$ is replaced by $\overline{\Phi}_1^{m'n'mn} = (1+\gamma)\overline{\Phi}^{m'n'mn}$.

Considering the modified extinction coefficient as:

$$\kappa_{em}^{mn} = \kappa_a + \kappa_s\frac{\kappa_s}{4\pi}\overline{\Phi}_1^{mnm'n'}\,\Delta\Omega^{mn} \tag{15}$$

the system of algebraic equations becomes:

$$\begin{aligned}&A_c D_{cr}^{mn} I_c^{mn} - A_w D_{cr}^{mn} I_w^{mn} + A_t D_{cz}^{mn} I_t^{mn} - A_b D_{cz}^{mn} I_b^{mn} \\ &\quad = -\kappa_{cm}^{mn}\Delta v\,\Delta\Omega^{mn} I_P^{mn} + S_{mP}^{mn}\Delta v\,\Delta\Omega^{mn} + (A_e - A_w) \\ &\qquad \times(\alpha_{mn+\frac{1}{2}} I_P^{mn+\frac{1}{2}} - \alpha_{mn-\frac{1}{2}} I_P^{mn-\frac{1}{2}})\end{aligned} \tag{16}$$

This system of algebraic equations has more unknowns than the number of equations. Therefore other equations must be introduced to relate the control volume facial intensity as well as the edge intensity of the angular range to the nodal intensity. The following simple step scheme is used to ensure positive intensity [10,13]:

For $D_{cr}^{mn} > 0$ and $D_{cz}^{mn} > 0$

$$I_e^{mn} = I_P^{mn} \tag{17a}$$

$$I_w^{mn} = I_W^{mn} \tag{17b}$$

$$I_t^{mn} = I_P^{mn} \tag{17c}$$

$$I_b^{mn} = I_B^{mn} \tag{17d}$$

$$I_P^{mn+\frac{1}{2}} = I_P^{mn} \tag{18a}$$

$$I_P^{mn-\frac{1}{2}} = I_P^{mn-1} \tag{18b}$$

with the condition: $I_P^{m\frac{1}{2}} = I_P^{m1}$ [20].

Rearranging Eq. (16) for I_P^{mn} and substituting Eq. (18a) for direction $mn+\frac{1}{2}$ results in:

$$I_P^{mn}=\frac{A_{\mathrm{w}}D_{\mathrm{cr}}^{mn}I_W^{mn}+A_{\mathrm{b}}D_{\mathrm{cz}}^{mn}I_B^{mn}-(A_{\mathrm{e}}-A_{\mathrm{w}})\alpha_{mn-\frac{1}{2}}I_P^{mn-\frac{1}{2}}+S_{mP}^{mn}\Delta V\Delta\Omega^{mn}}{(A_{\mathrm{e}}D_{\mathrm{cr}}^{mn}+A_{\mathrm{t}}D_{\mathrm{cz}}^{mn}-(A_{\mathrm{e}}-A_{\mathrm{w}})\alpha_{mn+\frac{1}{2}}+\kappa_{\mathrm{em}}^{mn}\Delta V\Delta\Omega^{mn})} \tag{19}$$

Eqs. (18a) and (18b) hold for all directions, while Eqs. (17a)–(17d) need to be rewritten as the direction cosines ($D_{\mathrm{cr}}^{mn}>0$ and $D_{\mathrm{cz}}^{mn}>0$) change sign.

4. Validation of numerical results

We have considered two cases of cylindrical enclosures whose walls are assumed black:

- Enclosure with an absorbing and emitting medium.
- Enclosure with scattering medium.

According to the symmetry condition along the z-axis, the centreline is treated as a fictious, perfectly specular reflecting boundary.

The results are presented in terms of normalized net radiative heat fluxes defined by:

$$Q_r^{\mathrm{r}}=\frac{1}{E_{\mathrm{b}}}\int_{\Omega=4\pi}(\vec{\Omega}\cdot\vec{e}_r)\,\mathrm{d}\Omega=\sum_{mn}I_P^{mn}D_{\mathrm{cr}}^{mn} \tag{20a}$$

$$Q_z^{\mathrm{r}}=\frac{1}{E_{\mathrm{b}}}\int_{\Omega-4\pi}(\vec{\Omega}\cdot\vec{e}_z)\,\mathrm{d}\Omega=\sum_{mn}I_P^{mn}D_{\mathrm{cz}}^{mn} \tag{20b}$$

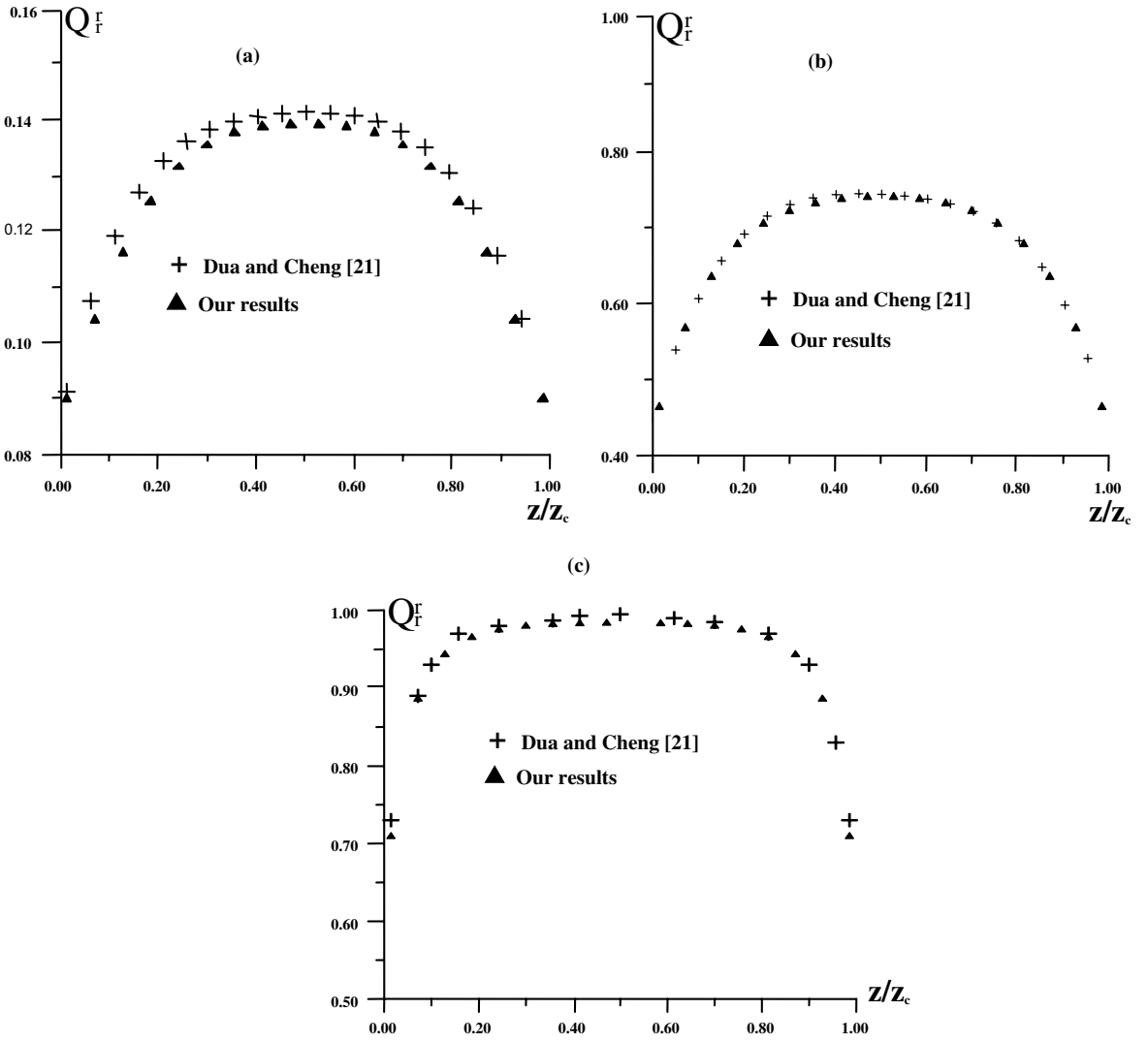

Fig. 4. Comparison of dimensionless radial radiative heat flux profiles at the lateral cylinder surface for three optical thickness (a) $\tau=0.1$, (b) $\tau=1$ and (c) $\tau=5$.

where the normalization constant E_b is the maximum emissive power, which is equal to σT_g^4 in the first test case (i.e. an absorbing–emitting medium) and equal to σT_h^4 in the second test case (i.e. a purely scattering medium).

These two problems are solved by the present FVM using expressions (10a) and (10b). In order to verify the validity of the established expressions (i.e. Eqs. (10a) and (10b)), comparisons are made with existing results [8,21].

4.1. Enclosure with absorbing–emitting medium

The first test case involves a cylindrical enclosure containing a homogeneous, absorbing–emitting medium maintained at constant temperature ($T_g = 100$ °C).The walls are assumed cold ($T_w = 0$ °C) and black ($\varepsilon_w = 1$). The cylinder dimensions are: height $z_c = 2$ m and radius $r_c = 1$ m.

The number of spatial control volumes used for this calculation is $(N_r \times N_z) = (15 \times 35)$. Because of the problem symmetry, the total solid angle 4π is divided into $(N_\theta \times \frac{N_\psi}{2}) = (6 \times 8)$ control solid angles which is analogous to the conventionnel S_{12} DOM in the number of radiation directions.

Fig. 4 shows a good agreement, especially for higher values of the optical thickness, between our results and the exact analytical solutions of radiative transfer in an absorbing, emitting medium in a cylinder obtained by Dua and Cheng [21]. Larger value of τ result in larger Q_r^* because emission is higher. Errors of up to ±5% in these exact results are expected because they were obtained by digitizing published plots. The discrepency between our results with the exact solutions obtained by [21] decrease with the optical thickness and this is due especially to the step scheme used here which become inaccurate in the case of small values of the optical thickness.

4.2. Purely scattering medium

The dimensions of the cylinder are height $z_c = 2$ m, radius $r_c = 1$ m. The lateral surface is the hot surface with $T_h = 100$ °C and the temperature of the bases is $T_c = 0$ °C.

The scattering phase function is approximated by a finite series of Legendre polynomial series as:

$$\Phi(\vec{\Omega} \to \vec{\Omega}') = \Phi(\cos\theta_P) = \sum_{j=0}^{N} C_j P_j \cos(\theta_P)$$

where θ_P is the scattering angle between the incoming direction $\vec{\Omega}'$ and the outgoing direction $\vec{\Omega}$ ($\cos\theta_P = \vec{\Omega}' \cdot \vec{\Omega}$). C_j's are the expansion coefficients and P_j is the Legendre polynomial of order j. The expansion coefficients in the case of forward-scattering (F_2 and F_3) and in the case of backward-scattering (B_2 and B_3) are presented in Table 1 [22].

The number of spatial control volumes used for this calculation is $(N_r \times N_z) = (15 \times 35)$ and the total solid angle 4π is divided into $(N_\theta \times \frac{N_\psi}{2}) = (6 \times 8)$.

Predictions of the non-dimensional heat flux distribution on the lateral area (Figs. 5–9) are shown for five different scattering conditions. As can be seen in these figures, the forward-scattering phase function F_2 transfers the most amount of radiation from the hot wall into the cold medium. The backward-scattering phase function B_1 transfers the least amount of radiative energy.

Table 1
Expansions coefficients in the phase function expansion [22]

J	F_1	F_2	F_3	B_1	B_2
0	1.00000	1.00000	1.00000	1.00000	1.00000
1	2.53602	2.00917	1.20000	−0.56524	−1.20000
2	3.56549	1.56339	0.50000	0.29783	0.50000
3	3.97976	0.67407		0.08571	
4	4.00292	0.22215		0.01003	
5	3.66401	0.04725		0.00063	
6	3.01601	0.00671			
7	1.23304	0.00068			
8	1.30351	0.00005			
9	0.53463				
10	0.20136				
11	0.05480				
12	0.01099				
N	13	9	3	6	3
$C_1/3$	0.84534	0.66972	0.40000	−0.18841	−0.40000

$N + 1$: number of terms in the phase function expansion, $C_1/3$: asymmetry factor.

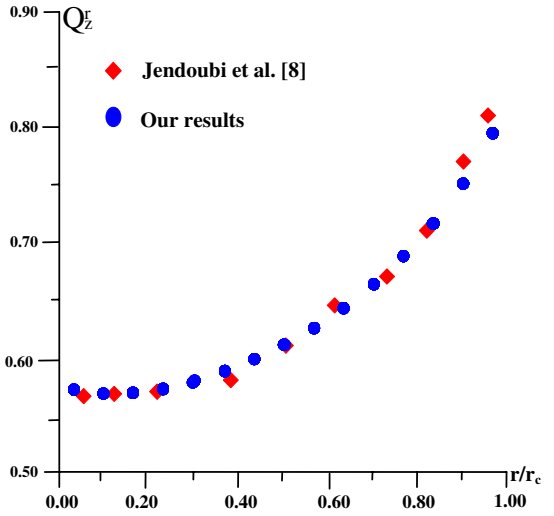

Fig. 5. Radiative flux profiles on bottom and top cylinder surfaces for isotropic scattering for purely diffusing medium case.

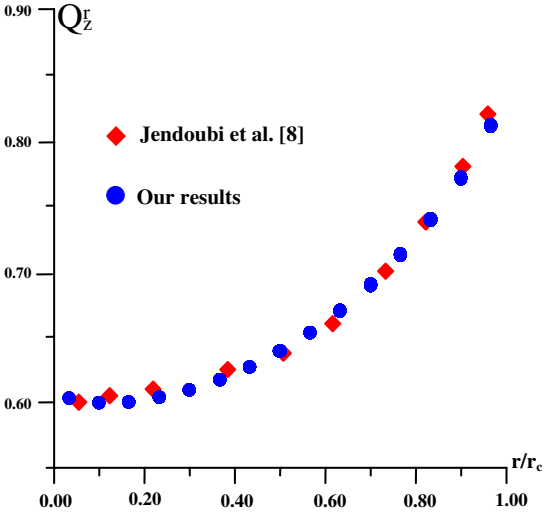

Fig. 6. Radiative flux profiles on bottom and top cylinder surfaces for B_1 scattering function for purely diffusing medium case.

Comparisons with the numerical results obtained by Jendoubi et al. [8] with the DOM shows a good agreement.

5. Concluding remarks

Explicit expressions for the coefficients appearing in the discretized ART have been determined using the

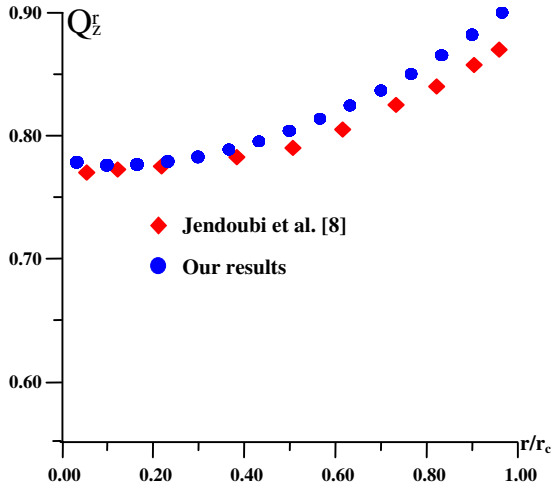

Fig. 7. Radiative flux profiles on bottom and top cylinder surfaces for F_2 scattering function for purely diffusing medium case.

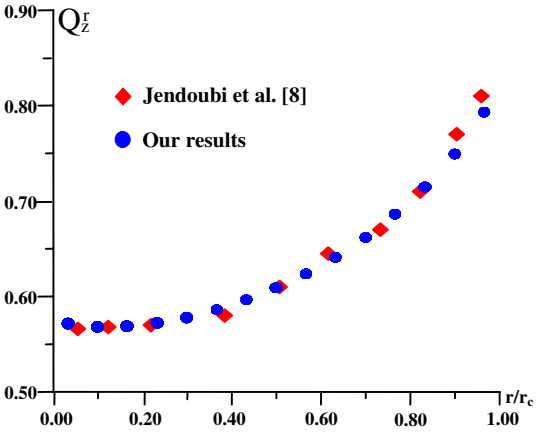

Fig. 8. Radiative flux profiles on bottom and top cylinder surfaces for B_2 scattering function for purely diffusing medium case.

FVM. These coefficients verify the recursive relation established by Carlson and Lathrop [14] and lead to accurate numerical results.

Appendix A

By assuming that the radiative intensity is constant on the east and the west control volume faces and in the solid control angle $\Delta\Omega^{mn}$, the development of the term (a) yields to:

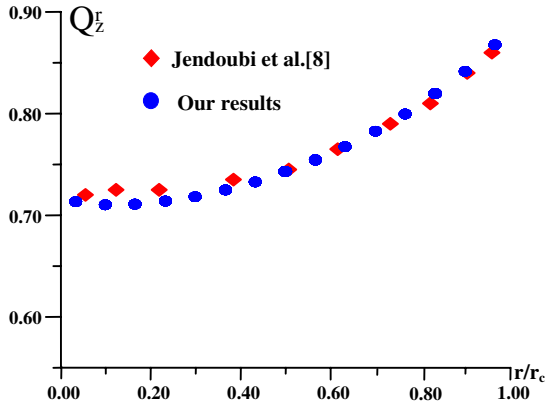

Fig. 9. Radiative flux profiles on bottom and top cylinder surfaces for F_3 scattering function for purely diffusing medium case.

$$\begin{aligned}
&\int_{\Delta v}\int_{\Delta\Omega^{mn}} \frac{1}{r}\frac{\partial}{\partial r}(rI\sin\theta\cos\psi)\,\mathrm{d}v\,\mathrm{d}\Omega \\
&\quad=\int_{\Delta\Omega^{mn}}\int_0^{2\pi}\int_{z_\mathrm{b}}^{z_\mathrm{t}}\int_{r_\mathrm{w}}^{r_\mathrm{e}} \frac{1}{r}\frac{\partial}{\partial r}(rI\sin\theta\cos\psi)r\,\mathrm{d}r\,\mathrm{d}\varphi\,\mathrm{d}z\,\mathrm{d}\Omega \\
&\quad=2\pi\Delta z(r_\mathrm{e}I_\mathrm{e}^{mn}-r_\mathrm{w}I_\mathrm{w}^{mn})\int_{\Delta\Omega^{mn}}\sin\theta\cos\psi\,\mathrm{d}\Omega \\
&\quad=2\pi\Delta z(r_\mathrm{e}I_\mathrm{e}^{mn}-r_\mathrm{w}I_\mathrm{w}^{mn})\int_{\Delta\Omega^{mn}}\vec{e}_r\cdot\vec{\Omega}^{mn}\,\mathrm{d}\Omega \\
&\quad=D_\mathrm{cr}^{mn}A_\mathrm{e}I_\mathrm{e}^{mn}-D_\mathrm{cr}^{mn}A_\mathrm{w}I_\mathrm{w}^{mn}
\end{aligned}$$

where $D_\mathrm{cr}^{mn}=\int_{\Delta\Omega^{mn}}(\vec{e}_r\cdot\vec{\Omega}^{mn})\,\mathrm{d}\Omega$ is the direction cosine in the r-direction and A_w and A_e are the areas of the west and east face of the control volume, respectively.

The development of the term (b) is also done by assuming that the radiative intensity is constant on the top and bottom control volume faces and within the control solid angle. Considering these assumptions, the term (b) will be written as:

$$\begin{aligned}
&\int_{\Delta v}\int_{\Delta\Omega^{mn}}\frac{\partial}{\partial z}(I\cos\theta)\,\mathrm{d}v\,\mathrm{d}\Omega \\
&\quad=\pi(r_\mathrm{e}^2-r_\mathrm{w}^2)(I_\mathrm{t}^{mn}-I_\mathrm{b}^{mn})\int_{\Delta\Omega^{mn}}\cos\theta\,\mathrm{d}\Omega \\
&\quad=\pi(r_\mathrm{e}^2-r_\mathrm{w}^2)(I_\mathrm{t}^{mn}-I_\mathrm{b}^{mn})D_\mathrm{cz}^{mn} \\
&\quad=D_\mathrm{cz}^{mn}A_\mathrm{t}I_\mathrm{t}^{mn}-D_\mathrm{cz}^{mn}A_\mathrm{b}I_\mathrm{b}^{mn}
\end{aligned}$$

where $D_\mathrm{cz}^{mn}=\int_{\Delta\Omega^{mn}}(\vec{e}_z\cdot\vec{\Omega}^{mn})\,\mathrm{d}\Omega$ is the direction cosine in the z-direction and A_t and A_b are respectively the area surfaces of the top and bottom face of the control volume, respectively.

The ART is developed by assuming that the radiative intensity is constant within the control volume and in the angle range $\lfloor\theta^{m-\frac{1}{2}},\theta^{m+\frac{1}{2}}\rfloor$. Taking into account these assumptions, the treatment of the term (c) leads to:

$$\begin{aligned}
&-\int_{\Delta v}\int_{\Delta\Omega^{mn}}\frac{1}{r}\frac{\partial}{\partial\psi}(I\sin\theta\sin\psi)\,\mathrm{d}v\,\mathrm{d}\Omega \\
&\quad=-2\pi\Delta z\Delta r\int_{\Delta\Omega^{mn}}\frac{\partial}{\partial\psi}(I\sin\theta\sin\psi)\sin\theta\,\mathrm{d}\theta\,\mathrm{d}\psi \\
&\quad=-(A_\mathrm{e}-A_\mathrm{w})\int_{\theta^{m-\frac{1}{2}}}^{\theta^{m+\frac{1}{2}}}\sin(\theta^2)(I_P^{mn+\frac{1}{2}}\sin\psi^{n+\frac{1}{2}}-I_P^{mn-\frac{1}{2}} \\
&\qquad\times\sin\psi^{n-\frac{1}{2}})\,\mathrm{d}\theta \\
&\quad=-(A_\mathrm{e}-A_\mathrm{w})\sin\psi^{n+\frac{1}{2}}\left\{\frac{\Delta\theta}{2}-\frac{1}{4}[\sin(2\theta^{m+\frac{1}{2}})\right. \\
&\qquad\left.-\sin(2\theta^{m-\frac{1}{2}})]\right\}I_P^{mn+\frac{1}{2}}+(A_\mathrm{e}-A_\mathrm{w})\sin\psi^{n-\frac{1}{2}}\left\{\frac{\Delta\theta}{2}\right. \\
&\qquad\left.-\frac{1}{4}[\sin(2\theta^{m+\frac{1}{2}})-\sin(2\theta^{m-\frac{1}{2}})]\right\}I_P^{mn-\frac{1}{2}} \\
&\quad=(A_\mathrm{e}-A_\mathrm{w})(\alpha_{mn+\frac{1}{2}}I_P^{mn+\frac{1}{2}}-\alpha_{mn-\frac{1}{2}}I_P^{mn-\frac{1}{2}})
\end{aligned}$$

where $\alpha_{mn\pm\frac{1}{2}}$ are coefficients of the ART defined as:

$$\begin{aligned}
\alpha_{mn+\frac{1}{2}}&=-\sin(\psi^{n+1/2})\left\{\frac{\Delta\theta}{2}-\frac{1}{4}[\sin(2\theta^{m+1/2})\right. \\
&\qquad\left.-\sin(2\theta^{m-1/2})]\right\} \\
\alpha_{mn-\frac{1}{2}}&=-\sin(\psi^{n-1/2})\left\{\frac{\Delta\theta}{2}-\frac{1}{4}[\sin(2\theta^{m+1/2})\right. \\
&\qquad\left.-\sin(2\theta^{m-1/2})]\right\}
\end{aligned}$$

The source term (d) is written as:

$$S=\kappa_\mathrm{a}(\vec{r})I^0(\vec{r})+\frac{\kappa_\mathrm{s}(\vec{r})}{4\pi}\int_{4\pi}I(\vec{r},\vec{\Omega}')\Phi(\vec{\Omega}'\to\vec{\Omega})\,\mathrm{d}\Omega'$$

The discretization of this term over a control volume and a control solid angle will give:

$$S_P^{mn}=\frac{\kappa_\mathrm{s}}{4\pi}I_P^{mn}\overline{\Phi}^{mnmn}\Delta\Omega^{mn}+S_{mp}^{mn}$$

with

$$S_{mp}^{mn}=\kappa_\mathrm{a}I^0(T)+\frac{\kappa_\mathrm{e}}{4\pi}\sum_{(m',n')\neq(m,n)}I_P^{m'n'}\overline{\Phi}^{m'n'mn}\Delta\Omega^{m'n'}$$

and

$$\overline{\Phi}^{m'n'mn}=\frac{1}{\Delta\Omega^{mn}\Delta\Omega^{m'n'}}\int_{\Delta\Omega^{m'n'}}\int_{\Delta\Omega^{mn}}\Phi(\vec{\Omega}'\to\vec{\Omega})\,\mathrm{d}\Omega\,\mathrm{d}\Omega'$$

The radiative intensity is herein also assumed constant within the control volume and the control solid angle.

References

[1] M. Permutter, J.R. Howell, Radiant transfer through a gray gas between concentric cylinders using monte carlo method, J. Heat Transfer 86 (1964) 165–179.

[2] T.M. Lows, H. Bartelds, M.P. Heamp, S. Michelfelder, B.E. Pai, in: N.H. Afgan, J.M. Beer (Eds.), Prediction of Radiant, Heat flux distribution, Heat Transfer in Flames, Scripta, Washington, 1974, pp. 179–190.
[3] F.R. Steward, K.N. Tennankore, Towards a finite difference solution coupled with the zone method for radiative transfer for a cylindrical combustion chamber, J. Inst. Energy (1979) 107–114.
[4] R. Fernandes, J. Francis, Combined conductive and radiative heat transfer in an absorbing, emitting, and scattering cylinder medium, J. Heat Transfer 104 (1982) 594–601.
[5] M.P. Mengüç, R. Viskanta, Radiative transfer in axisymmetric finite cylindrical enclosures, J. Heat Transfer 108 (1986) 271–276.
[6] S.T. Thynell, M.N. Özişik, Radiation transfer in absorbing, emitting, isotropically scattering, homogeneous cylindrical media, J. Quantitat. Spectrosc. Radiat. Transfer 38 (6) (1987) 413–426.
[7] W.A. Fiveland, A discrete ordinates method for predicting radiative heat transfer in axisymmetric enclosure, ASME, 1982, Paper 82-HT-20.
[8] S. Jendoubi, H.S. Lee, T.K. Kim, Discrete ordinates solutions for radiatively participating media in a cylindrical enclosure, J. Thermophys. Heat Transfer 7 (2) (1993), April to June.
[9] E.H. Chui, G.B. Raithby, Computation of radiant heat transfer on a nonorthogonal mesh using the finite-volume method, Numer. Heat Transfer, Part B 23 (1993) 269–288.
[10] E.H. Chui, G.D. Raithby, P.M. Hughes, Prediction of radiative transfer in cylindrical enclosures with the finite volume method, J. Thermophys. Heat Transfer 6 (4) (1992) 605–611.
[11] J.C. Chai, H.C. Lee, S.V. Patankar, Finite volume method for radiation heat transfer, J. Thermophys. Heat Transfer 8 (3) (1994) 419–425.
[12] J.P. Moder, J.C. Chai, G. Parthasarathy, U.S. Lee, S.V. Patankar, Non axisymmetric radiative transfer in cylindrical enclosures, Numer. Heat Transfer, Part B 30 (1996) 437–452.
[13] S.W. Baek, M.Y. Kim, Modification of the discrete ordinates method in an axisymmetric cylindrical geometry, Numer. Heat Transfer, Part B 31 (1997) 313–326.
[14] B.G. Carlson, K.D. Lathrop, in: H. Greenspan, C.N. Kelber, D. Okrent (Eds.), Computing Method in Reactors Physics, Gordon and Breach, New York, 1968, pp. 171–266.
[15] A.S. Jamaluddin, P.J. Smith, Predicting radiative transfer in axisymmetric cylindrical enclosures using the discrete ordinates method, Combust. Sci. Technol. 62 (1988) 173–186.
[16] S.R. Mathur, J.Y. Murthy, Radiative heat transfer in periodic geometries using a finite volume method, J. Heat Transfer 121 (1999) 357–364.
[17] J. Liu, H.M. Shang, Y.S. Chen, Development of an unstructured radiation model applicable for two-dimensional planar, axisymmetric, and three dimensional geometries, J. Quantitat. Spectrosc. Radiat. Transfer 66 (6) (2000) 17–33.
[18] R. Siegel, J.R. Howell, Thermal Radiation Heat Transfer, third ed., Hemisphere, New York, 1992, pp. 686–689.
[19] G.D. Raithby, E.H. Chui, A finite volume method for predicting radiant heat transfer in enclosure with participating media, J. Heat Transfer 112 (1990) 415–423.
[20] E.E. Lewis, W.F. Miller Jr., Computational Methods of Neutron Transport, John Wiley, New York, 1984.
[21] S.S. Dua, P. Cheng, Multidimensional radiative transfer in non isothermal cylindrical media with non isothermal bounding walls, Int. J. Heat Mass transfer 18 (1975) 40–144.
[22] T.-K. Kim, H. Lee, Effect of anisotropic scattering on radiative heat transfer in two-dimensional rectangular enclosure, Int. J. Heat Mass Transfer 31 (8) (1988) 1711–1721.